

NANO MICRO  
**small**

Supporting Information

for *Small*, DOI: 10.1002/smll.201403402

Microwave Enabled One-Pot, One-Step Fabrication and Nitrogen Doping of Holey Graphene Oxide for Catalytic Applications

Mehulkumar Patel, Wenchun Feng, Keerthi Savaram, M. Reza Khoshi, Ruiming Huang, Jing Sun, Emann Rabie, Carol Flach, Richard Mendelsohn, Eric Garfunkel, and Huixin He\*

Copyright WILEY-VCH Verlag GmbH & Co. KGaA, 69469 Weinheim, Germany, 2013.

Supporting Information

**Title:**

**Microwave Enabled One-Pot, One-Step Fabrication and Nitrogen Doping of Holey Graphene Oxide for Catalytic Applications.**

*Mehulkumar Patel<sup>1</sup>, Wenchun Feng<sup>2</sup>, Keerthi Savaram<sup>1</sup>, Mohammadreza Khoshi<sup>1</sup>, Ruiming Huang<sup>1</sup>, Jing Sun<sup>1</sup>, Emman Rabie<sup>1</sup>, Carol flach<sup>1</sup>, Richard Mendelsohn<sup>1</sup>, Eric Garfunkel<sup>3</sup>, Huixin He<sup>1\*</sup>*

<sup>1</sup>Chemistry Department, Rutgers University, Newark, NJ 07102; <sup>2</sup>Department of Chemical Engineering University of Michigan, Ann Arbor, MI 48109; <sup>3</sup>Department of Chemistry and Chemical Biology, Rutgers University, 610 Taylor Rd, Piscataway, NJ 08854.

\* Correspondence: huixinhe@rutgers.edu

**Supplemental Experimental results:**

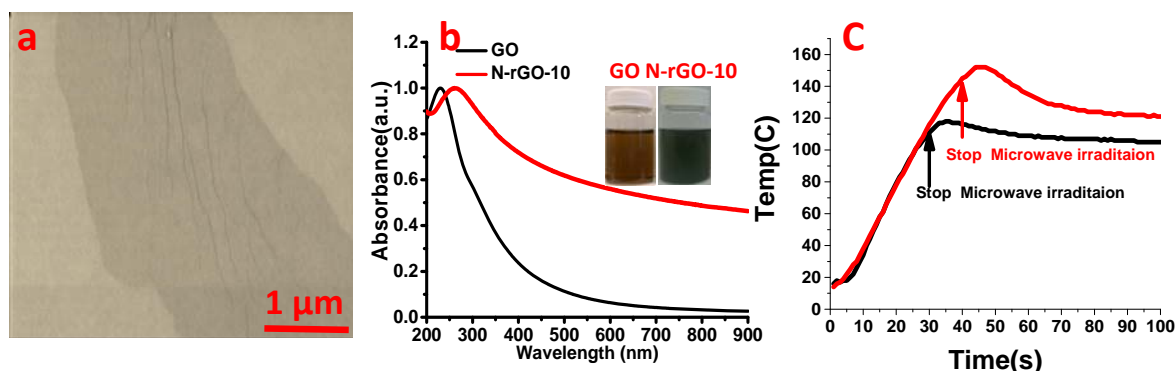


**Figure S1.**(a) STEM images of GO sheets obtained via 30 seconds of microwave heating. (b) UV-Vis-NIR spectra of GO sheets (black line) and N-rGO-10 (red line). Inset (b) is a digital picture of

an aqueous dispersion of GO (left) and N-rGO-10(right) shows different colors, indicating they are in different oxidation states. (c) is microwave heating temperature ( in Celsius) profile with time during GO and HGO synthesis.

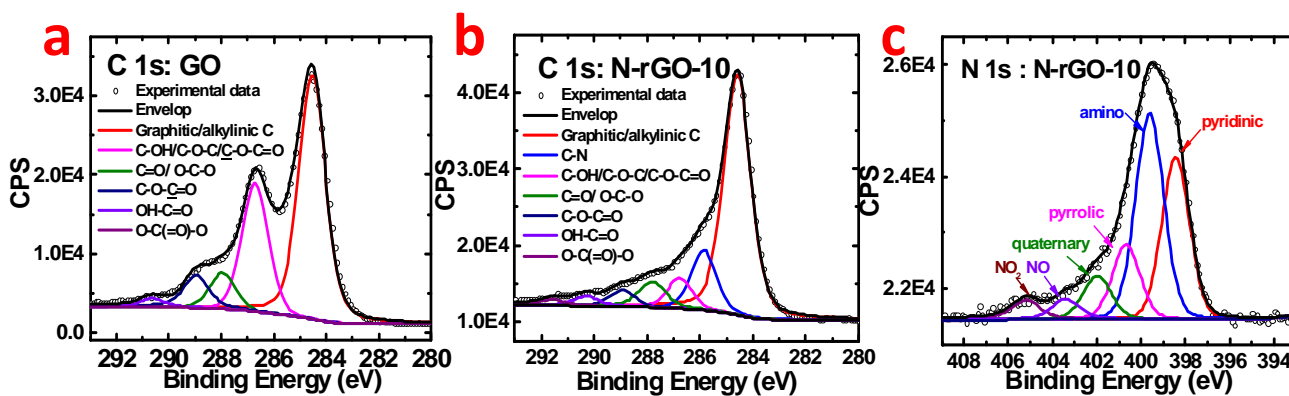


**Figure S2.** XPS high resolution C 1s peak analysis of GO (a) and N-rGO-10 (b). XPS high resolution N 1s peak analysis of N-rGO-10(c).

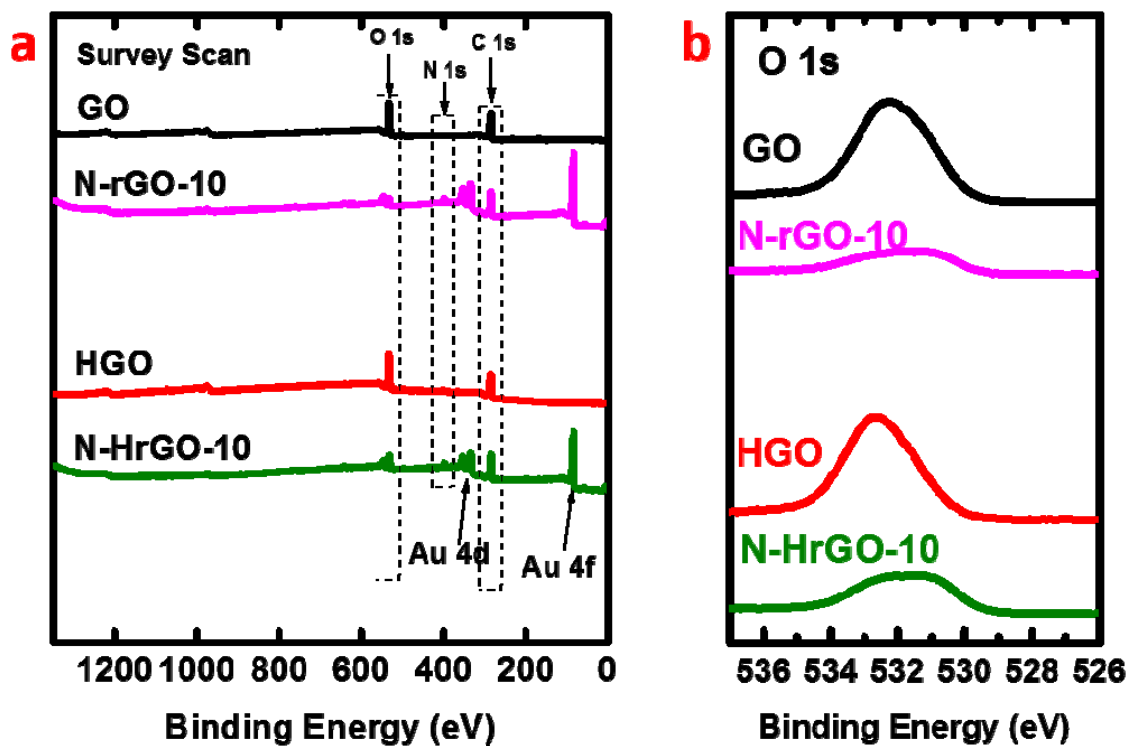


**Figure S3.** (a) XPS survey scan and (b) O 1s peak of GO, N-rGO-10, HGO and N-HrGO-10.

**Table S1:** Atomic ratio of C, N and O calculated from high resolution C 1s, N 1s and O 1s XPS peak analysis of different catalysts.

Samples	un-oxidizedC: oxidized C	N:C	C: O	% atomic N
GO	1.5	-	2.38	-
N-rGO-10	3.5	0.13	6.67	10.15%
HGO	1.5	-	2.38	-
N-HrGO-10	3.9	0.12	4.17	8.51%
N-HrGO-30	3.8	0.11	5.26	8.34%

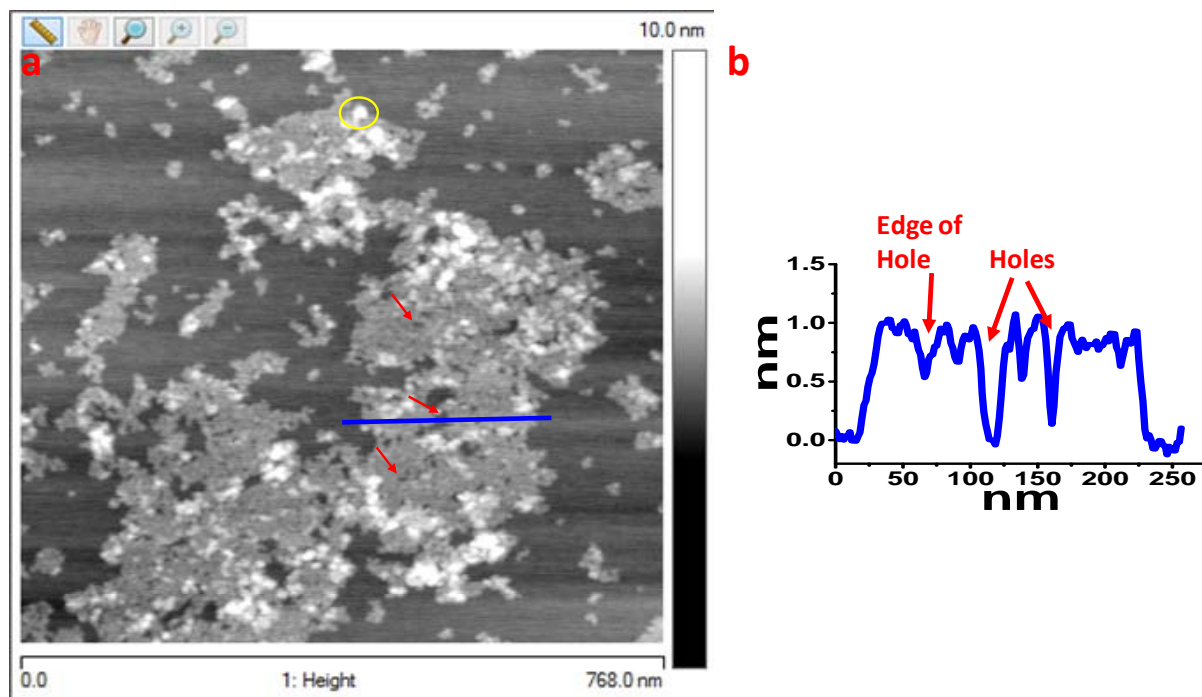


**Figure S4.** (a) A high magnification AFM image of HGO and (b) is the height section analysis of the blue line in HGO's AFM image (a). To easily see the nanoholes, red colored arrows were used to point some of them on a HGO sheet and a nanosized GO sheet sitting on a HGO sheet was circled with a yellow ring.

#### Surface area measurement of GO, HGO, N-rGO-10 and N-HrGO-10:

Methylene blue (MB) adsorption method is a common dye adsorption based approach used to determine the surface area of graphitic materials, with each mg of adsorbed methylene blue representing  $2.54\text{m}^2$  of surface area.<sup>[1]</sup> The surface area of graphene samples were calculated by adding a known mass of graphene sample into a standardized methylene blue solution (2mg/ml) in DI water. The solution was stirred for 24 hours to reach maximum adsorption of MB on the graphene samples. For each mg of graphene sample,  $750\mu\text{L}$  of MB (2mg/ml) is added so that the total mass of MB will remain 1.5 times higher than each of the graphene samples to reach a full coverage of MB on the graphene samples. The mixture was then centrifuged at 5000 rpm for 5

minutes to separate the non-absorbed MB molecules, which are still the supernatant. Then the MB concentration in the supernatant was determined by UV-vis spectroscopy at wavelength of 664 nm and compared to the initial standard concentration of MB prior to interacting with the graphene sample.

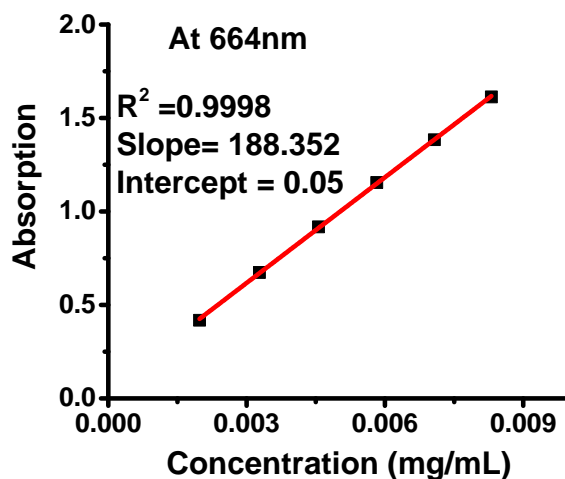


**Figure S5.** Linear relationships between the concentration of MB and its absorption at 664 nm.

**Table S2:-** The measured surface area of GO, HGO, N-rGO-10 and N-HrGO-10 via MB adsorption method.

Sample	Surface area(m <sup>2</sup> /g)
GO	947.55
HGO	1424.16
N-rGO-10	560.71
N-HrGO-10	1194.97

**TableS3:** Summary and comparison of chemical approaches to synthesise porous GO.

Ref.	Starting Material	Synthetic method	Chemicals involved	Synthetic procedure
<b>Our</b>	<b>Graphite</b>	<b>Microwave</b>	<b>HNO<sub>3</sub>, H<sub>2</sub>SO<sub>4</sub> and KMnO<sub>4</sub></b>	<b>300Watt, 40seconds</b>
[2]	GO	Chemical etching method	KMnO <sub>4</sub>	microwave 700W, 5minutes
[3]	GO	Enzymatic oxidation	Peroxidase + H <sub>2</sub> O <sub>2</sub>	Room temp, ~ 8- 10 days.
[4]	GO	Catalytic oxidation by metal + thermal annealing	Albumin, NaOH, gold nanoparticle, PEI modified quartz	90°C 2Hrs and 340°C, 2Hr
[5]	GO	Steam etching	Water	200°C for 5 to 20Hours.
[6]	GO	Chemical oxidation	Fuming HNO <sub>3</sub>	1 Hour- Bath sonication.
[7]	Reduced GO	Chemical Oxidation	HNO <sub>3</sub>	100°C, 4-11 hour
[8]	GO	Thermal treatment	CO <sub>2</sub>	250°C for 1Hour
[9]	GO	Hydrothermal+ thermal treatment	Biomass(PVA/resin), KOH, Ar gas	180°C, 12 Hour , 800°C for 1hour
[10]	Reduced GO	CVD/Thermal treatment	KOH , Ar Gas	800°C, 4 Hour
[11]	GO	Uv assisted etching	Uv(5mW/cm <sup>2</sup> ), ZnO nanorods	12 Hours
[12]	GO	Mesoporous substrate based	Nickel foam, PVP, Sulfonated polystyrene	400°C 2Hr and 800°C 2Hr
[13]	N doped rGO	Chemical + mechanical etching	KOH and Ball milling	42 Hours

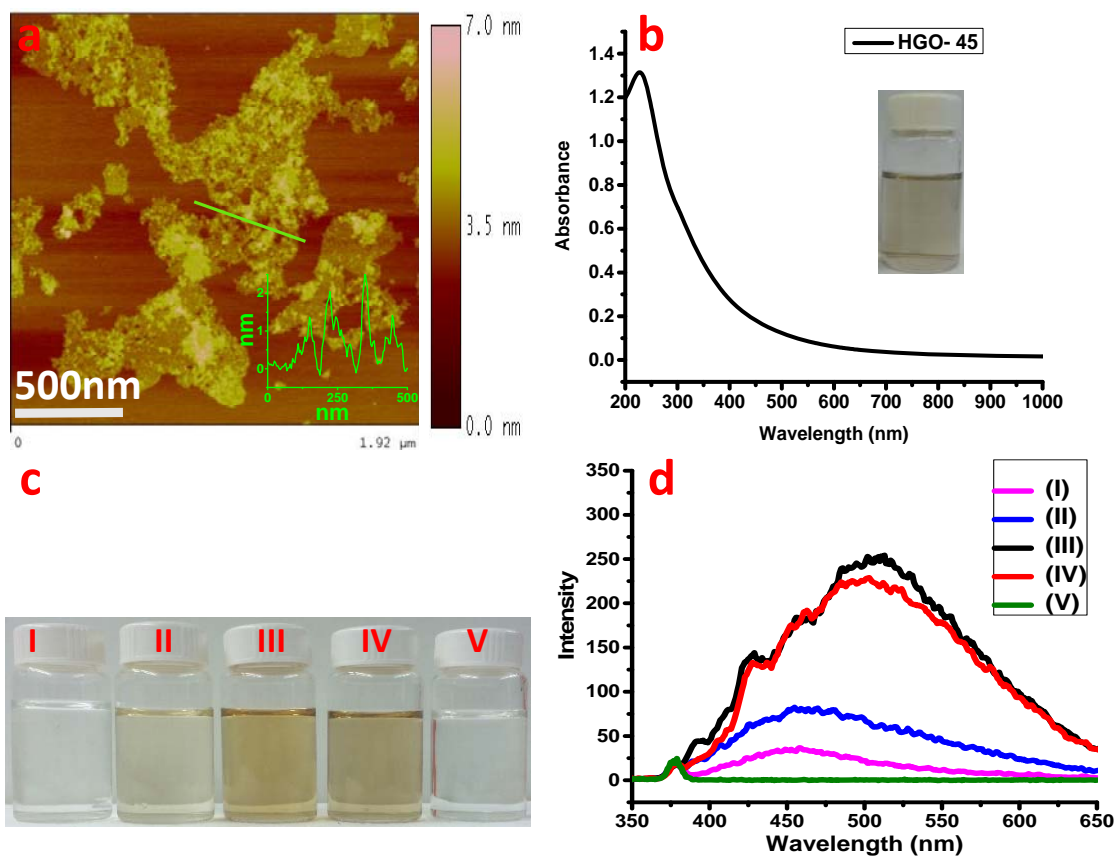


**Figure S6.**(a) AFM and (b) UV-Vis-NIR spectrum of an aqueous dispersion of HGO sheets obtained via 45seconds of microwave heating. The inset of (b) shows its digital picture. (c) is the digital pictures and (d) is the fluorescence emission spectra ( $\lambda_{\text{exc}} = 335\text{nm}$ ) of the filtrates, produced after graphite particles were oxidized with different microwave time: (I)30seconds, (II)40seconds, (III)45seconds, respectively. (IV) is the filtrate obtained with the same experimental conditions as (I), except that  $\text{KMnO}_4$  was excluded and (V) is the filtrate obtained with the same experiment condition as (II), except the graphite was excluded.



**Control Experiments to Support our proposed mechanism:**

Based on our proposed mechanism, the microwave heating, microwave irradiation time and  $\text{KMnO}_4$  playing very important roles in controlling the oxidation level and the morphology/structure of the fabricated graphene oxide sheets. We performed several control experiments to support our hypothesis. First we studied the effect of the amount of  $\text{KMnO}_4$  on graphene's morphology, size and oxidation level. For this aim we performed experiments with different amount of  $\text{KMnO}_4$  (0wt% and 125wt% of graphite) and kept all the other reagents ( $\text{H}_2\text{SO}_4$  and  $\text{HNO}_3$ ) and microwave condition (300Watt, 30 seconds) the same. When the  $\text{KMnO}_4$  is absent (0 wt% of graphite), we get uniform graphene nanosheets(**Figure S7a**) with the intrinsic property of graphene largely remained, consistent with our previous report.<sup>[14]</sup> The lateral size of the graphene nanosheets is around  $10 \pm 4$  nm from the AFM measurement (**Figure S7a**). The UV-Vis-NIR spectrum of the nanosheet solution(**Figure S7d-black line**) shows a peak at 264nm along with strong NIR absorption. However, when the amount of  $\text{KMnO}_4$  was increased to 125wt% of graphite, the lateral sizes of the product slightly increased ranging from tens of nanometers to hundreds of nanometers, as shown in its AFM images(**Figure S7b**). Moreover, the UV-visible spectrum (**Figure S7d-red line**) of the product shows a peak position at 240 nm, which indicates the product are partially oxidized compared to those obtained without  $\text{KMnO}_4$ . These results suggest that in absence of  $\text{KMnO}_4$ , the defect consumption rate is much faster than the rate of new defect generation, resulting in uniform nanosized graphene with largely retained intrinsic properties. But in the presence of  $\text{KMnO}_4$ , defect consumption speed is decreased possibly because the  $\text{MnO}_4^-$  ions anchor and /or bind to the defects (the oxygen containing functional groups generated in the first step of oxidation), which slows down the

speed of defect consumption. Hence the lateral size and oxidation level of graphene is slightly increased.

We also performed another control experiment to study the importance of microwave heating over traditional heating in HGO synthesis. In this control experiment, instead of microwave heating, we heated the mixture of graphite, sulfuric acid, nitric acid and  $\text{KMnO}_4$  (500wt% of graphite) at  $80^\circ\text{C}$  on oil bath for 12 hours. Similar to traditional Hummer's method, highly oxidized GO sheets (we referred as t-GO) were produced. The UV-Visible spectrum of the t-GO (**Figure S7d**-blue line) shows a typical absorption peak of GO at 230nm due to  $\pi \rightarrow \pi^*$  transition of  $\text{C}=\text{C}$  and a shoulder around 300nm due to  $n \rightarrow \pi^*$  transition of carbonyl functional groups(**Figure S7c**). The t-GO sheets are mainly single layered with their lateral sizes ranging from hundreds nanometers to a few micrometers. However, nanoholes in these sheets are seldom observed, suggesting that microwave heating is important to synthesis holey GO. This is possibly due to its ability to generate much higher local temperatures on the graphene surface, which enhances the defect dramatically consumption compared to the case of traditional heating.

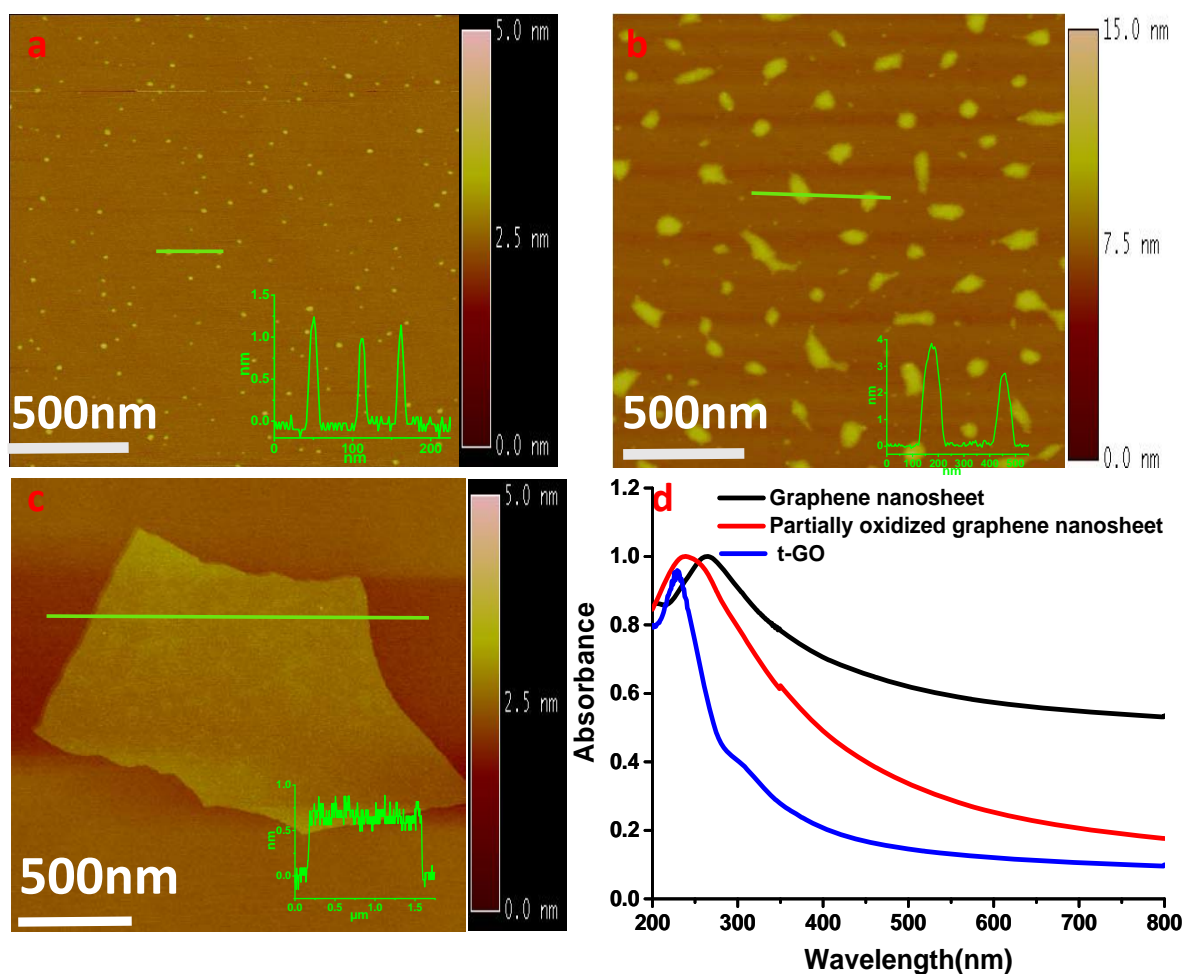


**Figure S7.** AFM images of the products obtained with different control experimental conditions. Microwave heating of the mixture of  $\text{H}_2\text{SO}_4$ ,  $\text{HNO}_3$  and graphite (300W and 30 seconds) in the absence of  $\text{KMnO}_4$  (a); in the presence of  $\text{KMnO}_4$  (125wt% of graphite) (b); traditional heating of the mixture of  $\text{H}_2\text{SO}_4$ ,  $\text{HNO}_3$  and graphite with  $\text{KMnO}_4$  (500wt% of graphite) (c). (d) shows their corresponding UV-VIS-NIR spectrum: black curve for (a), red curve for (b) and blue curve for (c). The UV peak at 264 nm and the strong NIR absorption indicate the intrinsic properties of graphene are largely maintained in product (a); the blue shift of the UV peak to 240 nm and the decrease in NIR absorption suggest that the product (b) is partially oxidized. The product (c) shows a typical UV-VIS-NIR spectrum of a highly oxidized graphene oxide.

**Table S4:** Summary of all published approach to synthesize N-doped graphene.

Ref.	Method	Chemicals	N-doping and reduction	N content (%)
<b>Our</b>	<b>Microwave</b>	<b>GO + NH<sub>4</sub>OH</b>	<b>120°C for 10 minutes</b>	<b>~8.5-10.5</b>
[15]	Hydrothermal + thermal	GO + melamine	180C, 12Hours and then at 800C,1 Hour	7.1-10.1
[13]	Hydrothermal	GO + NH <sub>4</sub> OH	180C for 12Hours	11.73
[16]	CVD	H <sub>2</sub> , Ethylene, diluted NH <sub>3</sub> in He, Cu foil	900C , 30 minutes	1.6-16
[17]	CVD	NH <sub>3</sub> , CH <sub>4</sub> , H <sub>2</sub> , Ar, Ni coated SiO <sub>2</sub>	1000C, 10minutes	4
[18]	Solvo thermal	Li <sub>3</sub> N/CCl <sub>4</sub> or N <sub>3</sub> C <sub>3</sub> Cl <sub>3</sub> /Li <sub>3</sub> N/CCl <sub>4</sub> , N <sub>2</sub> gas	250 – 50C, 6-10Hr	4.5-16.4
[19]	Thermal/ CVD	GO+ NH <sub>3</sub> /H <sub>2</sub>	800 to 1000C for 10minutes	2-2.8
[20, 21]	Plasma treatment	GO + N <sub>2</sub> plasma	1050C for 20minutes <sup>[20]</sup> or 30minutes <sup>[21]</sup>	8.5 <sup>[20]</sup> 3 <sup>[21]</sup>
[22]	CVD	GO+ NH <sub>3</sub> gas , Ar Gas	1000C (15C/minutes) for up to 2hour	---
[23]	pyrolysis	Dicyndiamine+FeCl <sub>2</sub> .4H <sub>2</sub> O+COCl <sub>2</sub> .6H <sub>2</sub> O	900C, 3Hours	3.6
[24]	Bottom up/template method	Ni foam, CH <sub>4</sub> gas, NH <sub>3</sub> gas, Ar gas, HF	1000C for 35minutes	3.1
[25]	CVD based thermal treatment	GO + melamine+ colloidal silica+ Ar gas	900 °C for 1 Hour	5.1

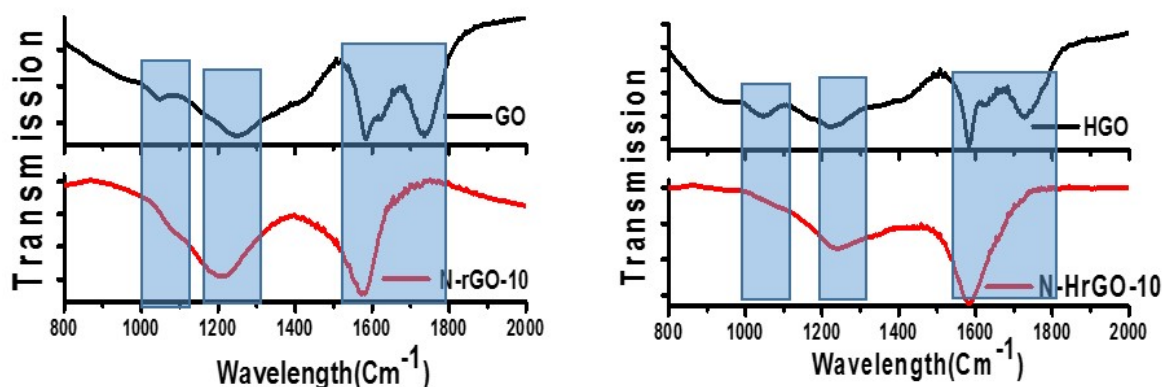


**Figure S8.** (a) FTIR spectrum of GO and N-rGO-10. (b) FTIR spectrum of HGO and N-HrGO-10.

**Table S5:** The calculated relative % of different kind of carbon from XPS high resolution C1s deconvolution in different catalysts.

Catalyst	C=C	C-OH	C=O	COOH
GO	48.92	23.73	6.76	7.10
N-rGO-10	63.60	8.33	7.18	3.97
HGO	46.07	23.40	7.47	7.89
N-HrGO-10	65.43	7.89	7.00	3.19

**Table S6:** Relative % ratio of different kind of N-dopant in N-HrGO-10, N-HrGO-30 and N-rGO-10.

N-Type (%)	Pyridinic N	Amino N	PyrrolicN	QuaternaryN	Other Oxidized N
N-HrGO-10	37.03	33.54	15.21	6.73	7.47
N-HrGO-30	35.97	35.61	13.91	6.47	8.04
N-rGO-10	29.36	38.72	14.19	8.47	9.25

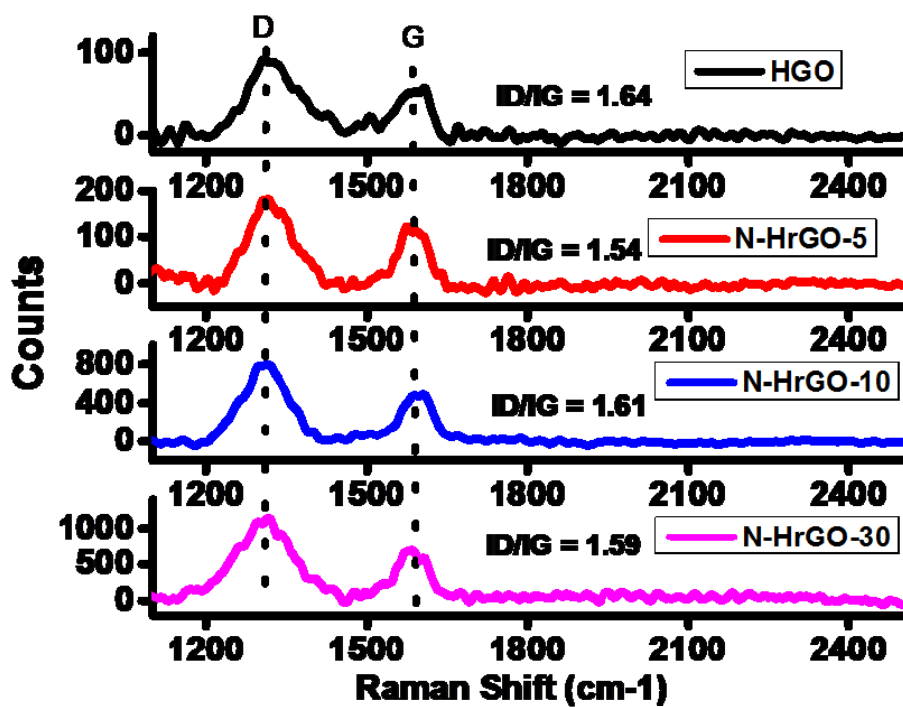
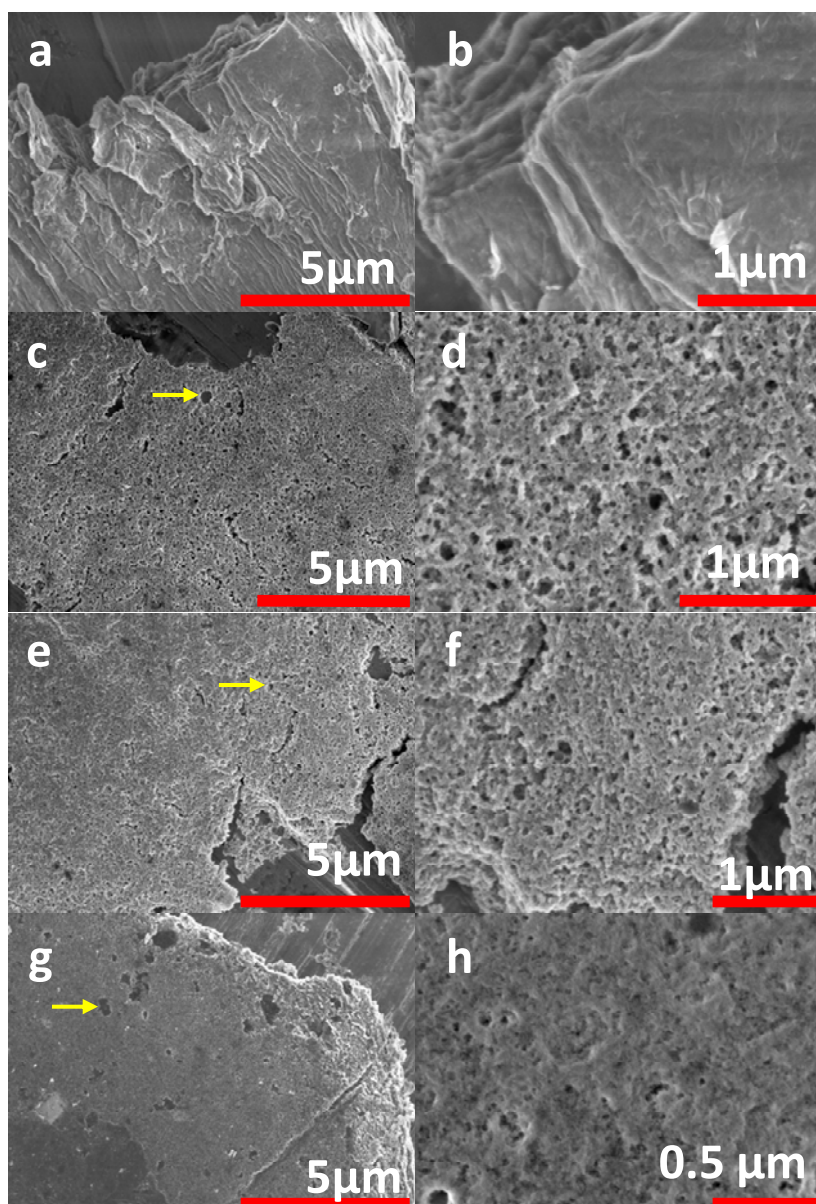
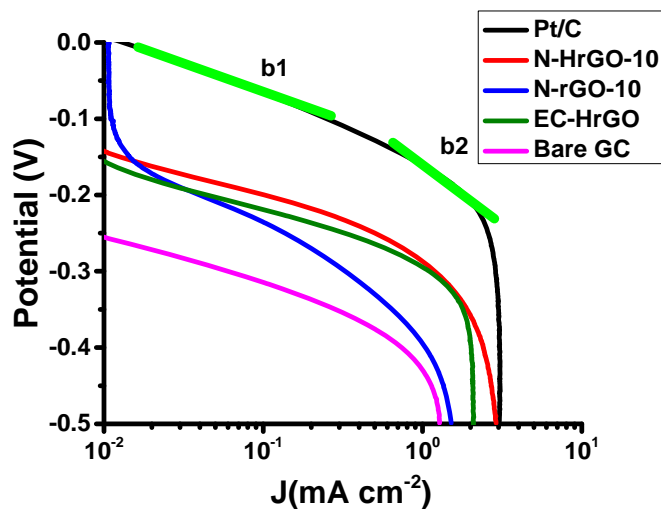


Figure S9. Raman spectra of HGO and N-HrGO-5, N-HrGO-10 and N-HrGO-30.



**Figure S10.** Scanning electron microscopic (SEM) images of N-rGO-10 (a and b), N-HrGO-5 (c and d), N-HrGO-10 (e and f) and N-HrGO-30 (g and h). The yellow arrow shows hole on N-HrGO's surface.



**Figure S11:** Tafel plots of Pt/C, N-HrGO-10, N-rGO-10, EC-HrGO and bare electrode derived by the mass-transport correction of corresponding RDE data (Figure 3C).

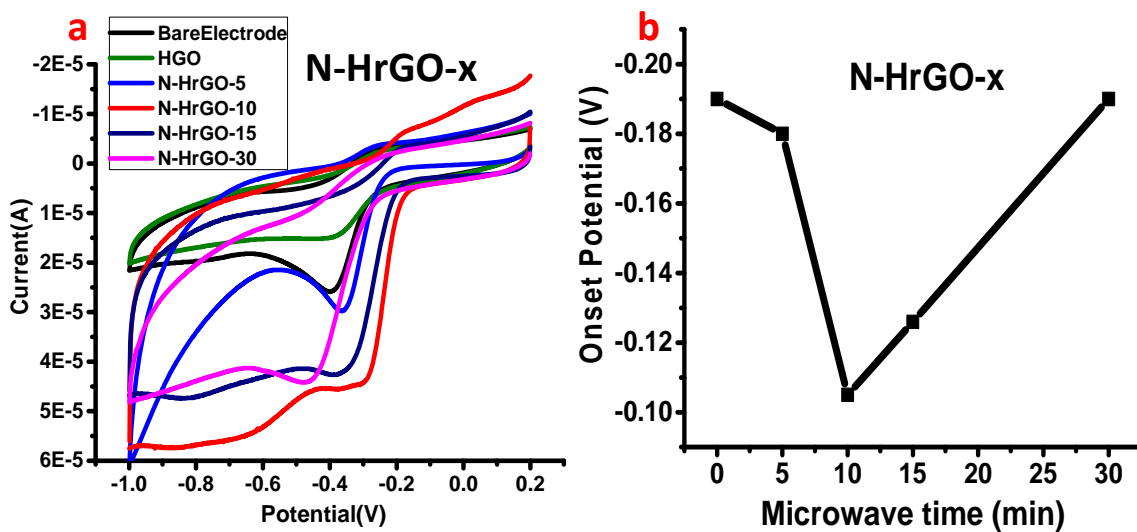


**Figure S12.** CV curves (a) and onset potential (b) of N-HrGO-*x* electrode in O<sub>2</sub> saturated 0.1M KOH electrolyte at a scan rate of 50mV/s, where “*x*” is different microwave time (0, 5, 10, 15, 30 minutes) used for synthesis of different N-HrGO. All potentials are measured using Ag/AgCl as a reference electrode.



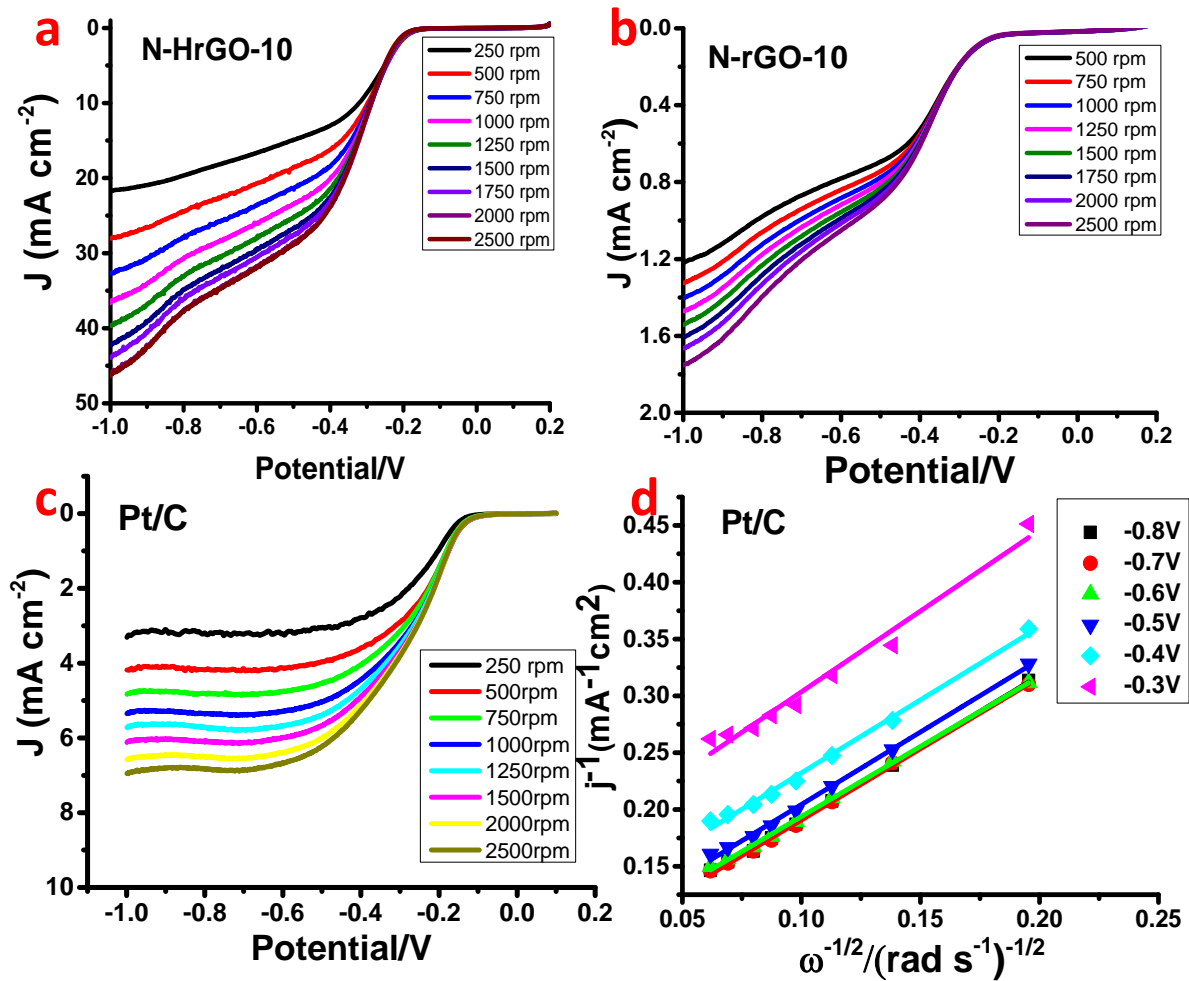


**Figure S13.** LSV curves of N-HrGO-10(a), N-rGO-10(b) and Pt/C(c) at different rotation speed in O<sub>2</sub> saturated 0.1M KOH solution at 10mV/s. (d) is K-L plot of Pt/C, obtained based on the LSV data(c). All potentials are measured using Ag/AgCl as a reference electrode.

References:

- [1] McAllister, M. J.; Li, J.-L.; Adamson, D. H.; Schniepp, H. C.; Abdala, A. A.; Liu, J.; Herrera-Alonso, M.; Milius, D. L.; Car, R.; Prud'homme, R. K., *Chemistry of Materials* **2007**, *19* (18), 4396.
- [2] Fan, Z.; Zhao, Q.; Li, T.; Yan, J.; Ren, Y.; Feng, J.; Wei, T., *Carbon* **2012**, *50* (4), 1699.
- [3] Kotchey, G. P.; Allen, B. L.; Vedala, H.; Yanamala, N.; Kapralov, A. A.; Tyurina, Y. Y.; Klein-Seetharaman, J.; Kagan, V. E.; Star, A., *ACS Nano* **2011**, *5* (3), 2098.

- [4] Xi, Q.; Chen, X.; Evans, D. G.; Yang, W., *Langmuir* **2012**,*28* (25), 9885.
- [5] Han, T. H.; Huang, Y. K.; Tan, A. T.; Dravid, V. P.; Huang, J., *J. Am. Chem. Soc.* **2011**,*133* (39), 15264.
- [6] Zhao, X.; Hayner, C. M.; Kung, M. C.; Kung, H. H., *ACS Nano* **2011**,*5* (11), 8739.
- [7] Wang, X.; Jiao, L.; Sheng, K.; Li, C.; Dai, L.; Shi, G., *Sci. Rep.* **2013**,*3*.
- [8] Peng, W.; Liu, S.; Sun, H.; Yao, Y.; Zhi, L.; Wang, S., *J. Mater. Chem. A* **2013**,*1* (19), 5854.
- [9] Zhang, L.; Zhang, F.; Yang, X.; Long, G.; Wu, Y.; Zhang, T.; Leng, K.; Huang, Y.; Ma, Y.; Yu, A., *Sci. Rep.* **2013**,*3*.
- [10] Zhu, Y.; Murali, S.; Stoller, M. D.; Ganesh, K. J.; Cai, W.; Ferreira, P. J.; Pirkle, A.; Wallace, R. M.; Cychosz, K. A.; Thommes, M.; Su, D.; Stach, E. A.; Ruoff, R. S., *Science* **2011**,*332* (6037), 1537.
- [11] Akhavan, O., *ACS Nano* **2010**,*4* (7), 4174.
- [12] Wang, Z.-L.; Xu, D.; Wang, H.-G.; Wu, Z.; Zhang, X.-B., *ACS nano* **2013**,*7* (3), 2422.
- [13] Jiang, Z. Q.; Jiang, Z. J.; Tian, X. N.; Chen, W. H., *J. Mater. Chem. A* **2014**,*2* (2), 441.
- [14] Patel, M. A.; Yang, H.; Chiu, P. L.; Mastrogiovanni, D. D.; Flach, C. R.; Savaram, K.; Gomez, L.; Hemnarine, A.; Mendelsohn, R.; Garfunkel, E.; Jiang, H.; He, H., *ACS Nano* **2013**,*7* (9), 8147.
- [15] Jiang, Z.-j.; Jiang, Z.; Chen, W., *J. Power Sources* **2014**,*251*, 55.
- [16] Luo, Z.; Lim, S.; Tian, Z.; Shang, J.; Lai, L.; MacDonald, B.; Fu, C.; Shen, Z.; Yu, T.; Lin, J., *J. Mater. Chem.* **2011**,*21* (22), 8038.
- [17] Qu, L. T.; Liu, Y.; Baek, J. B.; Dai, L. M., *Acs Nano* **2010**,*4* (3), 1321.
- [18] Deng, D. H.; Pan, X. L.; Yu, L. A.; Cui, Y.; Jiang, Y. P.; Qi, J.; Li, W. X.; Fu, Q. A.; Ma, X. C.; Xue, Q. K.; Sun, G. Q.; Bao, X. H., *Chemistry of Materials* **2011**,*23* (5), 1188.
- [19] Geng, D.; Chen, Y.; Chen, Y.; Li, Y.; Li, R.; Sun, X.; Ye, S.; Knights, S., *Energy Environ. Sci.* **2011**,*4* (3), 760.
- [20] Shao, Y.; Zhang, S.; Engelhard, M. H.; Li, G.; Shao, G.; Wang, Y.; Liu, J.; Aksay, I. A.; Lin, Y., *J. Mater. Chem.* **2010**,*20* (35), 7491.
- [21] Jafri, R. I.; Rajalakshmi, N.; Ramaprabhu, S., *J. Mater. Chem.* **2010**,*20* (34), 7114.
- [22] Wang, S.; Zhang, L.; Xia, Z.; Roy, A.; Chang, D. W.; Baek, J. B.; Dai, L., *Angew. Chem., Int. Ed.* **2012**,*51* (17), 4209.
- [23] Choi, C. H.; Park, S. H.; Woo, S. I., *ACS nano* **2012**,*6* (8), 7084.
- [24] Xue, Y.; Yu, D.; Dai, L.; Wang, R.; Li, D.; Roy, A.; Lu, F.; Chen, H.; Liu, Y.; Qu, J., *Phys. Chem. Chem. Phys.* **2013**,*15* (29), 12220.
- [25] Liang, J.; Jiao, Y.; Jaroniec, M.; Qiao, S. Z., *Angew. Chem., Int. Ed.* **2012**,*51* (46), 11496.